

# Rainfall-triggered landslides in an unsaturated soil: a laboratory flume study

Mohammad Ahmadi-adli<sup>1</sup> · Nejan Huvaj<sup>1</sup> · Nabi Kartal Toker<sup>1</sup>

Received: 12 February 2017 / Accepted: 11 October 2017 / Published online: 28 October 2017  
© Springer-Verlag GmbH Germany 2017

**Abstract** Extreme and/or prolonged rainfall events frequently cause landslides in many parts of the world. In this study, infiltration of rainfall into an unsaturated soil slope and triggering of landslides is studied through laboratory model (flume) tests, with the goal of obtaining the triggering rainfall intensity–duration ( $I$ – $D$ ) threshold. Flume tests with fine sand at two different relative densities (34 and 48%) and at slope angle of  $56.5^\circ$  are prepared, and rainfall (intensity in the range of 18 to 64 mm/h) is applied via a mist sprinkler system to trigger landslides. Soil water characteristic curve and hydraulic conductivity function of the fine sand are also presented. In flume tests, suction in the soil is measured with tensiometers, the progress of wetting front with time and deformations in the soil are also measured. Some of the findings of this study are: for the fine sand used in this study (a) the failure mechanism is infinite-slope type (mostly translational), and the failure surface is generally coincident with the wetting front or is in its vicinity, (b) the deformations leading to a landslide occurred abruptly, (c) both relatively high-intensity–short-duration rainfalls and relatively low-intensity–long duration rainfalls triggered landslides, (d) the shape of the  $I$ – $D$  threshold is demonstrated to be a bilinear relation in log intensity–log duration plot, (e) below a certain rainfall

intensity landslides are not triggered, (f) the effect of relative density of the soil on the  $I$ – $D$  threshold is demonstrated by physical laboratory tests (as the relative density of the soil increases, the triggering rainfall intensity–duration threshold moves to larger rainfall events). The results of this study could be useful for accurate numerical modeling of rainfall-triggered landslides.

**Keywords** Rainfall-triggered landslides · Infiltration · Unsaturated soil · Soil–water characteristic curve · Slope stability

## Introduction

Extreme and/or prolonged rainfall events frequently cause landslides in many parts of the world (Nadim et al. 2009; Toll et al. 2011; Lu and Godt 2013) as well as in Turkey (Fig. 1). Rainfall-triggered landslide develops due to wetting of an unsaturated soil, which increases the moisture content, decreases the suction in the ground, reduces the shear strength of the soil, leading to deformations in the slope (Fig. 2). Modeling of rainfall infiltration, seepage, and slope stability is quite complex for unsaturated soils, since it is controlled by many variables such as the characteristics of the rainfall and the nonlinear hydraulic and mechanical constitutive properties of the unsaturated soil.

For early warning and to predict the time and location of rainfall-triggered landslides, rainfall intensity–duration ( $I$ – $D$ ) threshold is frequently used. Rainfall thresholds (global, national, or for a specific region) are commonly defined by statistically evaluating and curve-fitting to data obtained from archives of past rainfall events that

✉ Nejan Huvaj  
nejan@metu.edu.tr

Mohammad Ahmadi-adli  
ahmadiadli@gmail.com

Nabi Kartal Toker  
tokar@metu.edu.tr

<sup>1</sup> Civil Engineering Department, METU, ODTU,  
06800 Ankara, Turkey



**Fig. 1** **a** Aerial view of numerous shallow landslides after an intense rainfall in the city of Rize, Turkey, **b** damage due to landslide after heavy rainfall in Rize, northern Turkey, in August 2010

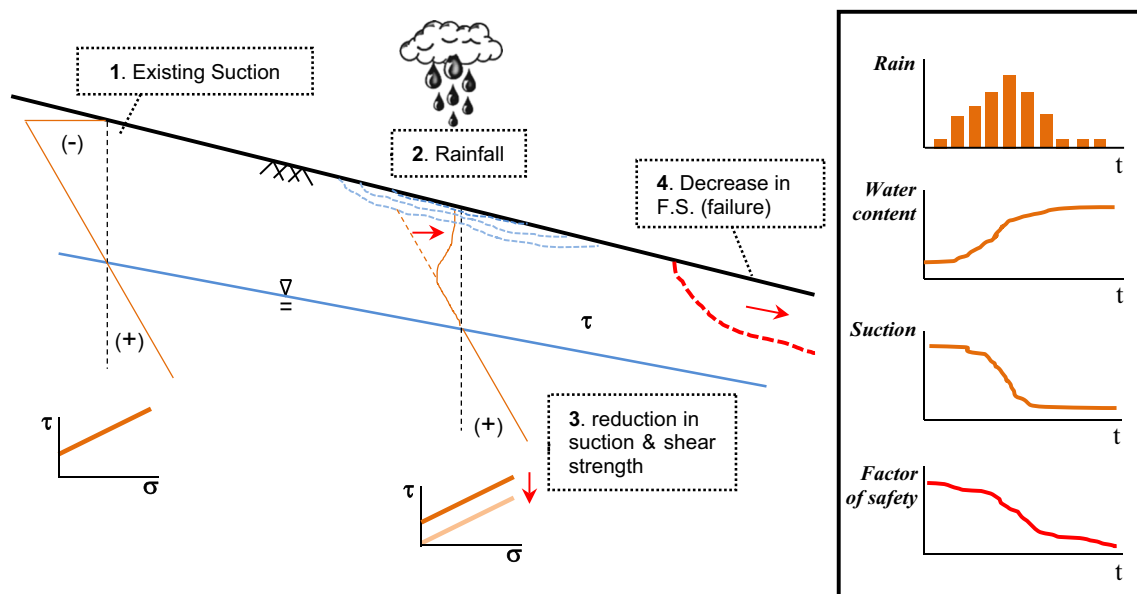


**Fig. 2** Conceptual illustration of the processes leading to failure in rainfall-triggered landslides in unsaturated soils (Ahmadi-adli 2014)

triggered landslides (Caine 1980; Jibson 1989; Reichenbach et al. 1998, Hong et al. 2006; Guzzetti et al. 2007; van Westen et al. 2007; Chen and Wang 2007; Guzzetti et al. 2008; Rossi et al. 2010; Lu and Godt 2013; Vennari et al. 2014). Examples of  $I$ - $D$  thresholds reported in the literature are presented in Fig. 3, rainfalls below the threshold line do not trigger landslides.

Another approach to the rainfall-triggered landslide problem is numerical modeling that considers the physical mechanism of slope failure either by uncoupled infiltration and slope stability studies (some of them using simple infinite slope stability factor of safety calculation and applying it spatially via geographic information systems) or by deformation-coupled infiltration and slope stability studies (Alonso et al. 1990; Iverson et al. 1997; Montgomery et al. 1997; Crosta and Frattini 2003;

Rahimi et al. 2011; Lu et al. 2012; Eichenberger et al. 2013). Infiltration and stability are very sensitive to model boundary conditions, initial conditions, and unsaturated soil properties. The current state of the art is focusing on improvement of numerical analysis methods and on implementation of different unsaturated soil plasticity rules in coupled analyses. In general, the number of coupled numerical studies is rather limited, and further verification studies are needed. The current physical model study can be used for verification purposes in numerical studies.

There are a number of field-scale tests studying the rainfall-induced landslides each investigating different aspect/mechanism (e.g., Moriwaki et al. 2004; Rahardjo et al. 2008; Godt et al. 2009; Askarinejad 2013; Springman et al. 2013). Field studies use extensive

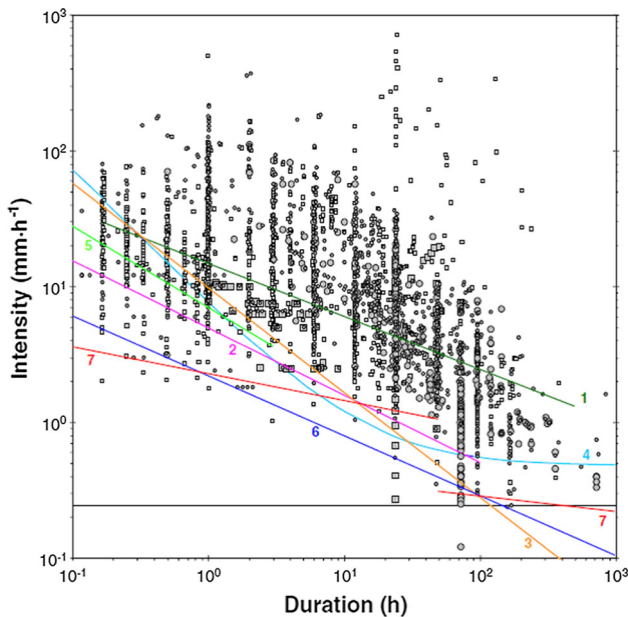


**Fig. 3** Global *I–D* thresholds (1) Caine (1980); (2) Innes (1983); (3) Clarizia et al. (1996); (4) Crosta and Frattini (2001); (5) Cannon and Gartner (2005); (6) using entire data set, Guzzetti et al. (2008); and (7) using probability estimates of rainfall conditions, Guzzetti et al. (2008), horizontal line shows 0.25 mm/h (figure from Guzzetti et al. 2008)

instrumentation to measure the hydromechanical response of soils in slopes to rainfall events and develop an understanding of the failure mechanisms. Laboratory physical model (flume) experiments are also used to model the behavior of unsaturated slopes. The reason why laboratory model tests are preferred to study the physical phenomenon is that, in a controlled environment and uniformly prepared/well-known soil conditions, the mechanism can be studied without being influenced by other unknown factors/variabilities in nature, and numerical studies can be conducted for the measurements in laboratory model tests. Many have conducted laboratory 1-g flume experiments, mostly on sandy material, subjected to rainfall and investigated pre-failure and post-failure behavior and failure mechanisms (Wang and Sassa 2001, 2003; Damiano 2004; Lourenco et al. 2006; Picarelli et al. 2006; Montrasio and Valentino 2007; Olivares et al. 2009; Fang et al. 2012; Zhou et al. 2013; Okada 2014; Wu et al. 2015). Laboratory flume model tests are also used for investigation of sediment discharge and impact of rising water level on rainfall-induced shallow landslides (e.g., Tohari et al. 2007; Acharya et al. 2009; Schnellmann et al. 2010). Some of the flume studies are listed in Table 1. It should be noted that there is no scaling of the real-life problem in the flume tests. In the current study, the results of laboratory flume experiments are used to develop *I–D* threshold and to investigate the effect of soil relative density on it.

## Experimental study

### Material used

Soil used in the current study is uniformly graded fine sand with 3% non-plastic fines. Grain size distribution (ASTM D6913), the specific gravity of solids ( $G_s$ ) (ASTM D854), minimum/maximum void ratio, density in a dry state (ASTM D4253 and D4254), and saturated hydraulic conductivity (ASTM D2434) of this soil are listed in Table 2.

Wetting soil–water characteristic curve (SWCC) of the soil (at different dry densities) is assessed using capillary column method (Richards 1931) (Fig. 4a). Hydraulic conductivity function (HCF) is determined using infiltration column method (ASTM D7664) (Fig. 4b).

### Laboratory flume setup

To study the infiltration and triggering of slope instability, laboratory model experiments in flume setup are conducted with the application of artificial rainfall having a known intensity. The flume box size, slope angle, and material properties in this study are determined to reflect the typical dimensions and material properties of real rainfall-triggered shallow landslides in Turkey. In addition, the following are considered: the typical depth/length ratio of rainfall-triggered landslides in Turkey, dimensions of the previous flume boxes used by other researchers in the literature, the time it will take to prepare soil sample in the box, the uniformity of the prepared soil sample in relation to its size and the time it will take to trigger landslide in the flume size selected. Figure 5 shows the schematic of the flume setup, which consists of a flume box, raising system, and adjustable raining system with mist sprinklers. The flume box can be tilted to desired inclinations (up to 55° from horizontal). The internal dimensions of the box are 187 cm (length) × 48 cm (width) × 70 cm (height). Two long rectangular faces of the box are made of tempered glass for allowing observations. Instrumentation used in this study are (i) miniature tensiometers (abbreviated as TNS) (Soilmoisture 2100F) to measure suctions in the range of 0–90 kPa, (ii) miniature pore pressure transducer (Druck PDCR-81 by PROCON Systems Inc.) to measure positive and negative pore pressures (PDCR), (iii) in-house-developed miniature inclinometers (elastic woven and rubber strips) to detect slope deformations, and (iv) digital cameras to obtain a video recording of deformations. Tensiometers and pressure transducers are inserted through an array of 12-mm-diameter holes on one of the long (glass) faces of the flume box. Inclinometers were placed at the side and at the center of the slope. Side inclinometers were made of 5-mm-wide black elastic

**Table 1** Some of the landslide-triggering experiments in the laboratory (flume and centrifuge tests)

References	Soil type	Rainfall intensity (mm/h)	Instrumentation	Slope angle (°)	Failure mechanism	Slope shape
Okura et al. (2002)	Sand	100	PPT, RG	10 and 32	“Fluidization”	
Take et al. (2004) (Centrifuge)	Fine and coarse granite sand	4.2 (250)	PPT, PIV	45	Static liquefaction	
Orense et al. (2004)	Omigawa sand	42–72	TDR	40	“Fluidization”	
Tohari et al. (2007)	River sand and granite sand	0–100	PPT	32–45	Rising water table	
Montrasio and Valentiono (2007)	Pyroclastic soils	84	TDR, PPT	38	Rising water table	
Olivares et al. (2009)	Pumice and fly ash	18–105	T/PPT/RG	0–40	Static liquefaction	
Huang and Yuin (2010)	Silty sand	47	T/RG/PPT/TDR	29 and 30	Rising water table	
Schnellmann et al. 2010	Well-graded sand with silt	40	TDR	33	–	
Askarinejad (2013) (Centrifuge)	Silty fine sand	1.27–2.5 (10–45)	TDR/T/PPT/PIV	38	Bottom-up effect	

*P* piezometer, *T* tensiometer, *PPT* pore pressure transducer, *RG* rain gauge, *TDR* time domain reflectometry, and *PIV* particle image velocimetry

**Table 2** Properties of the soil used in this study

$D_{10}$ (mm):	0.09	Coefficient of curvature, $C_c$ :	1.08	$\rho_{d \max}$ (g/cm <sup>3</sup> ):	1.648
$D_{30}$ (mm):	0.14	Coefficient of uniformity, $C_u$ :	2.24	$\rho_{d \min}$ (g/cm <sup>3</sup> ):	1.332
$D_{50}$ (mm):	0.18	Fines content (%):	3	$e_{\min}$ :	0.616
$D_{60}$ (mm):	0.202	USCS Soil Classification:	SP	$e_{\max}$ :	1.536
$G_s$ :	2.663	$k_{\text{sat}}$ (m/s):	$1.145 \times 10^{-6}$		

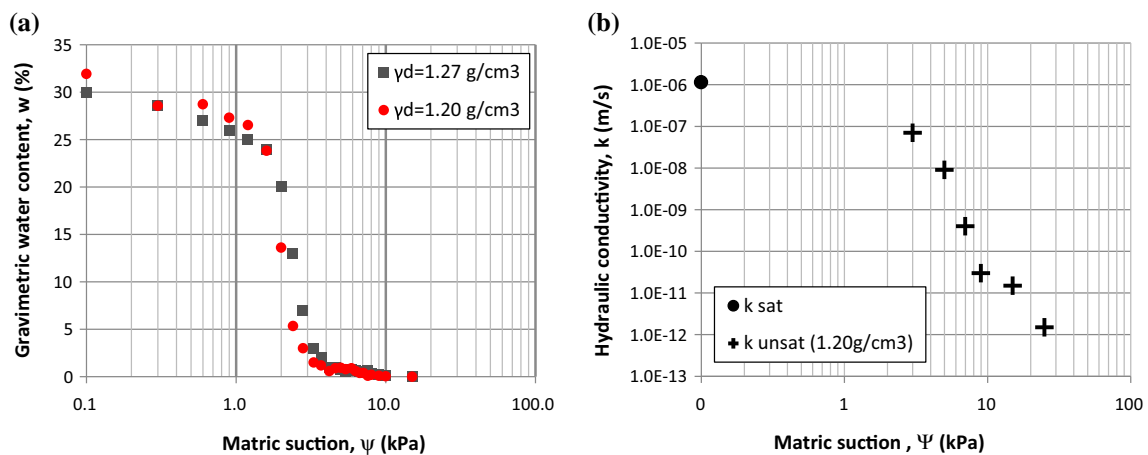


**Fig. 4** **a** Wetting SWCCs of the soil at different dry densities and **b** hydraulic conductivity of the soil obtained from infiltration column test

bands/strips with white ink-marks for measurement stations at 5-cm vertical spacing, and central inclinometers were made of very thin and very flexible (diameter: 1.0 mm) elastic strings with one tiny knot at measurement stations at

5-cm vertical spacing. The rainfall system consists of a control box (composed of the digital control panel, a spraying-resting control circuit, water reservoir, and actuators) and sprinkler array. Sprinkler array, which supports

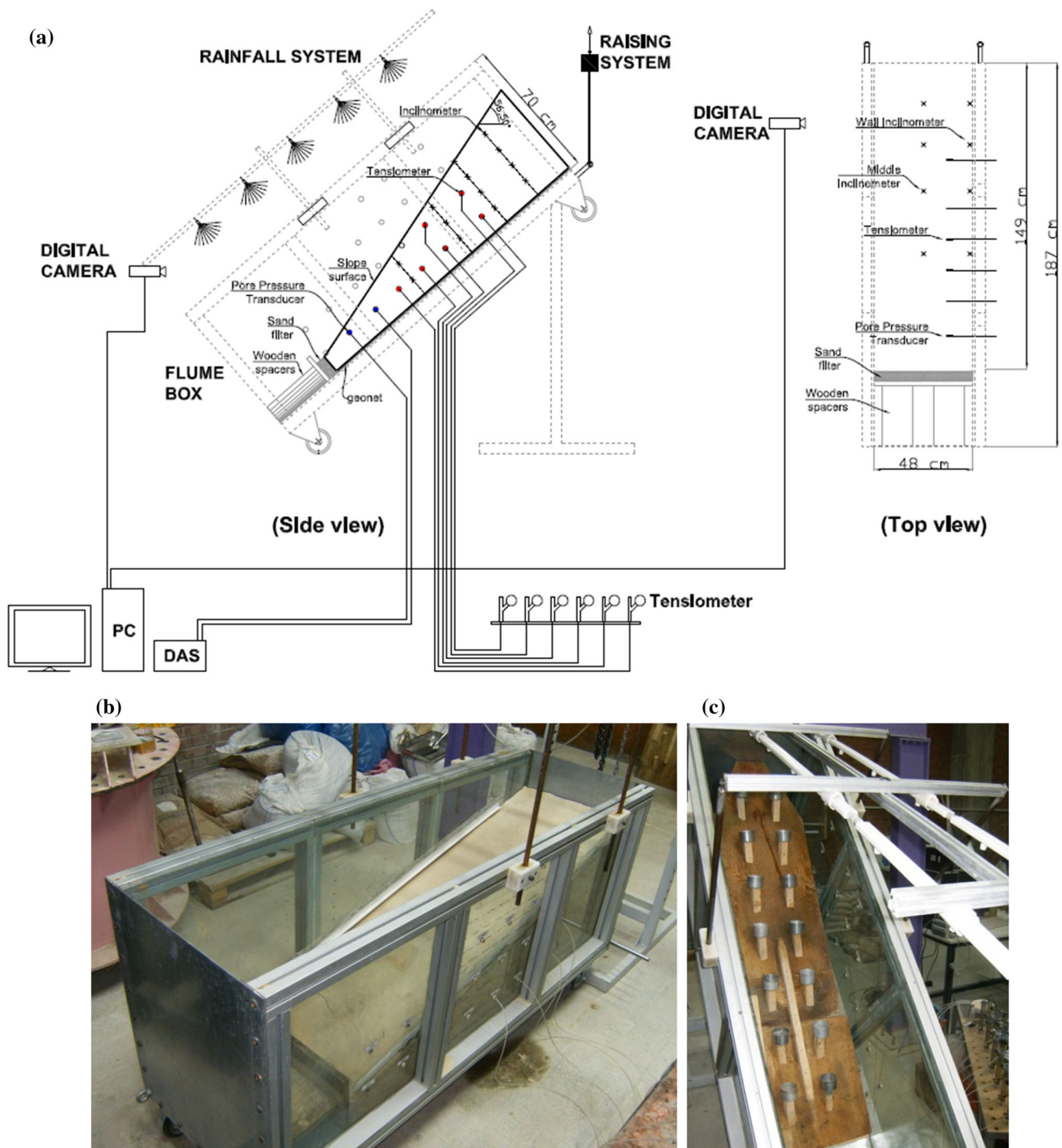


**Fig. 5** **a** Schematic drawing, **b** photo of the of the flume setup, and **c** photo of the mist sprinkler array and a preliminary test checking the uniformity of rainfall intensity over the slope

pressurized water hoses and nozzles, is mounted on a frame with adjustable elevation and inclination. Nozzles spray water at constant flow rate for an adjustable number of seconds per minute, which creates constant rainfall intensities when averaged over each minute. Rainfall is not applied as distinct rain droplets of a certain size, since this

would cause surface erosion and deformation due to impact energy of the raindrops, rather the rainfall is applied as a mist. In the experiments, surface erosion or deformation due to impact by raindrops is not observed. The system is capable of applying average rainfall intensities in the range

of 4–70 mm/h uniformly over the model slope (Ahmadi-adli 2014).

### Testing program

In total, 10 flume experiments are performed each with different constant rainfall intensities. In each experiment, slope failure time is recorded in order to create threshold  $I$ – $D$  plot. Variation of suction at each instrument location, wetting front progression over time, and deformation measurements by inclinometers at the end of the experiment are also recorded. In the flume experiments, soil specimens are prepared at two relative densities of 34 and 48% corresponding to 1.20 and 1.27 g/cm<sup>3</sup> dry densities, respectively. The basis for two different relative densities is that the rainfall-triggered landslides in Turkey occur in loose to medium dense soils ( $D_r$  less than 50%); we do not see rainfall-triggered landslides in dense soils. Slope surface inclination in all flume experiments is 56.5° from horizontal. The slope angle is a typical slope angle we observe in rainfall-triggered landslides in Turkey. Applied rainfall intensities range from 18 mm/h (relatively low) to 63.5 mm/h (relatively high) intensities.

### Sample preparation

Sample preparation is both the most important and the most sensitive part of laboratory flume tests (Fig. 6). The initial water content of sand is determined such that, when the sand gets wet, the volume of the sand, i.e., the initial dry density, does not change significantly and the sand can be easily placed and shaped. Sand is placed at an initial moisture content of 1.5%, in layers of about 5-cm thickness and compacted to target density by tamping on a steel plate that is placed on the layer surface. The toe of the soil slope in the flume experiments is a drainage boundary, created by placing a granular filter material wrapped in filter paper (Fig. 6a). The bottom boundary of the flume box is impervious; however, a geonet drainage material is placed at the bottom of the box to provide an interface between the soil and the base of the box (Fig. 6a). A water discharge hole exists in the box to prevent accumulation of water at the toe of the slope. Rainfall-triggered landslides in Turkey occur in slopes where the groundwater table is at a deep location, the soil being in unsaturated condition, and landslide is triggered before the wetting front reaching to the groundwater level located at deeper depths. Therefore, the lower boundary of the box is chosen to be far enough so that it would not influence the depth of failure surfaces, and in fact, all failures took place before the wetting front reaching to the bottom boundary (Fig. 11). Sample preparation steps are as follows:

- Placement of drainable filter toe boundary and central inclinometers (Fig. 6a).
- Soil placement in layers and compaction to the desired density. The most difficult and time-consuming part is carefully compacting soil in the vicinity of instrumentation such as central inclinometers or tensiometers (Fig. 6b). Before placement of a new 5-cm-thick soil layer, finished soil layer surface is scarified to establish interlocking of layers and to prevent any possible slip through layer boundaries. While placing the soil, tensiometers and pore pressure transducers are also placed in planned locations (Fig. 6b). The uniformity of soil placement is controlled in trial tests, measuring the density of the soil using small containers placed inside the soil while it is being prepared. For all tests,  $\pm 3\%$  tolerance in soil density was controlled.
- Trimming the slope face and giving it the final shape/angle (Fig. 6c–6d).
- Droplet drain installation on the side walls of the flume box. Rainfall system applies precipitation in the form of mist. When mist comes in contact with glass side walls of the flume box, it turns into water droplets that flow downward along the glass. This is considered as potential for increased infiltration along the side glass surfaces where observations of the wetting front are made. As a solution, 1.8-cm-wide plastic channels were prepared and attached to side glass walls, 10 cm above the soil surface, to drain away water drops along the sides.
- Covering—in order to avoid sample surface desiccation at the time between sample preparation and testing, nylon covers are placed over the soil slope surface (blue nylon cover in Fig. 6e). Another nylon cover is placed over the sprinkler array to keep all rainfall mist inside the flume system without evaporation (transparent nylon cover in Fig. 6e).
- Tilting the flume box to the desired angle—Immediately after sample preparation and covering, the flume specimen is carefully brought to the inclination desired using the lifting system (Fig. 6e).
- Suction equalization (equilibration) stage—the flume specimens were left for about 24 h before rainfall application, for equalization of suction values inside the soil sample. The 24 h duration is decided based on suction observations in the preliminary tests and deemed adequate. This stage is needed in order to get rid of any localized water accumulation and to balance initial water content distribution due to elevation head, which changes after tilting.



**Fig. 6** **a** Filter material located at the toe of the slope and geonet at the bottom boundary of the flume, **b** central and side inclinometers (hanging from wooden bars above the flume throughout soil placement) and miniature tensiometer placement (tensiometers are placed at two different locations: one group near the glass face of

flume box and another group at the middle of the flume) at different elevations and locations. **c** Sample; **d** after trimming, and **e** tilting of the flume specimen and tempering it for 24 h for suction equalization

**Testing**

At the beginning of the testing stage, nylon cover on the soil slope inside flume is removed. Testing stage is the continuous application of rainfall of constant intensity while measuring the suction at multiple locations in the soil and the recording of the progression of the wetting front with time. Rainfall application is continued until a landslide is triggered. At the end of the test, the failure surface and depth of failure are also recorded, by observing the side inclinometers and by digging out the coordinates of the measuring stations of the central inclinometers.

**Results**

**Test results**

Test results obtained from each flume experiment are (i) suction-time response at specific points, (ii) wetting front progress with time, and (iii) deformations and failure surface at the time of failure (Fig. 7). The time zero in the experiments is the time of start of rainfall application, and “time to failure” is defined as the time from the beginning of rainfall application until when the slope failure is observed (under continuous rainfall).

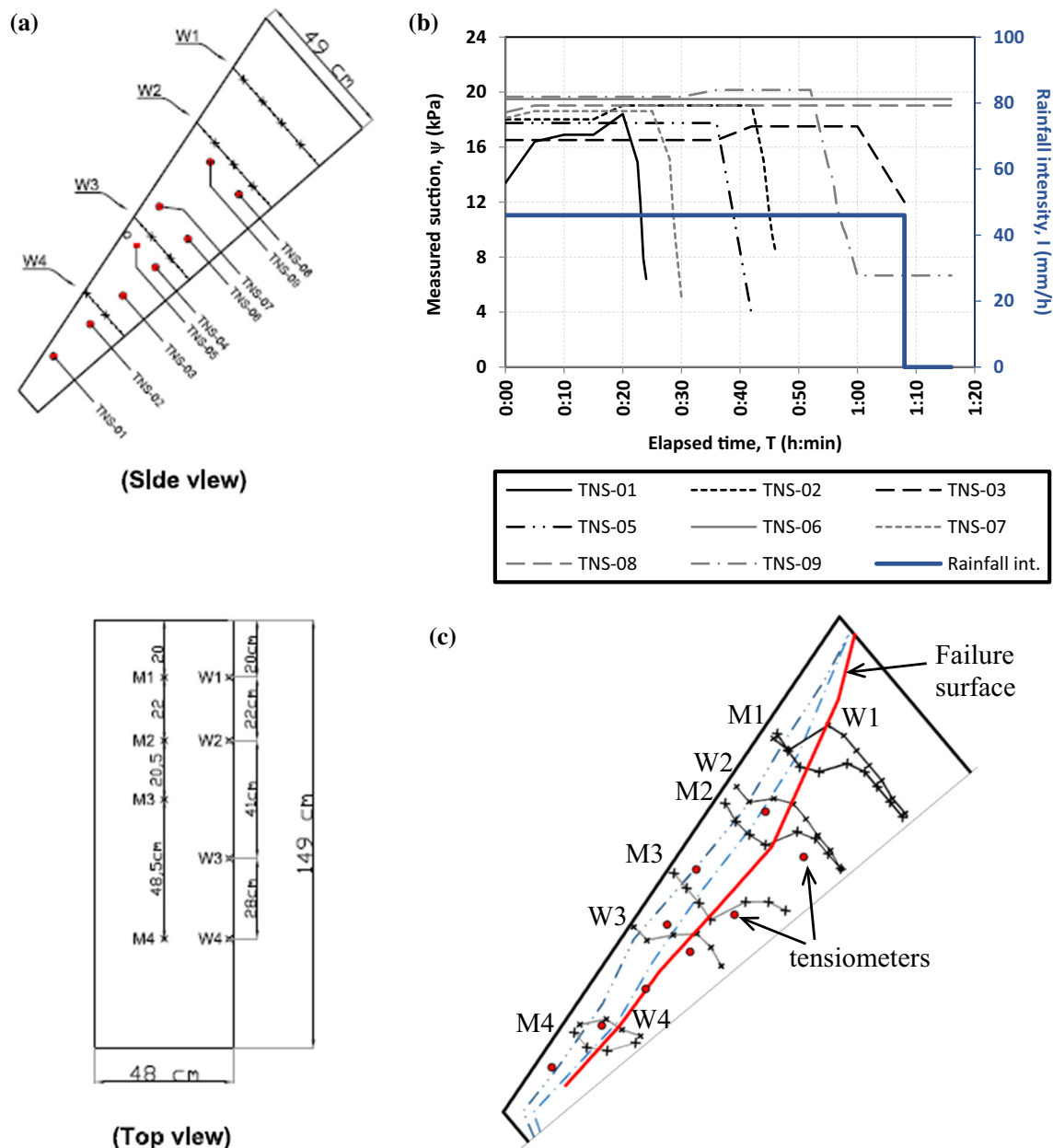


**Fig. 7** **a** Location of tensiometers and inclinometers in FLM\_04 test, **b** suction response after start of constant rainfall (46.3 mm/h), and **c** progress of wetting front (blue lines) with time, throughout the test

As an example, suction response recorded in the soil at different locations in the FLM\_04 test is plotted with time after the start of raining in Fig. 7b. The initial suction in the sample at different locations is measured in the range of 16.5 to 19.7 kPa before rainfall. The 46.3 mm/h rainfall infiltrates into the soil; the suction values drop as the wetting front reaches to the level of each tensiometer. The earliest response is seen at TNS-01 and the latest response at TNS-03, which is at the deepest location from the slope face. Recordings in TNS-06 and TNS-08 start at suction values of 19–19.5 kPa and stay constant throughout the test

and inclinometer loci after failure and emerging failure surface (TNS tensiometers, *M* middle inclinometer, and *W* wall inclinometer)

since failure occurs and the test ends before the water reaches to the depth of these tensiometers, during the total rainfall duration of one hour and eight minutes.

In order to assess the progress of wetting front with time in flume tests, the vertical distance between the wetting front (i.e., the depth in the soil where the water reaches and suction drops to zero) and the base of the flume setup is recorded from the glass side of the flume box at certain time intervals.

Figure 7c shows the progress of wetting front with time for FLM\_04 flume experiment. The failure is observed at



68 min after the start of rainfall at a depth of about 15 cm from ground surface at the deepest location. It is noticed that when the failure occurred the wetting front was at the depth of failure surface. Figure 8b shows, at the time of failure, 9-cm translational movement took place at the crest.

**Discussion of test results**

The suction response in the soil at different locations in the tests are plotted with time after the start of rainfall in Fig. 9 ( $D_r = 34\%$ ) and Fig. 10 ( $D_r = 48\%$ ). In the tests with  $D_r = 34\%$  (FLM\_03, 04, 05, 06, 08 and 13) except tests FLM\_03 and FLM\_13, measured initial suction values at tensiometers before rainfall are in the range of 17–21 kPa. At tests FLM\_03 and FLM\_13, slightly higher initial suctions are observed because of longer equalization time. Generally, in all tests, tensiometers TNS-1, 2, 5, and 7, which are located at shallower depths, show a drop in suction before the tensiometers at deeper locations do and then a slope failure is observed. But in tests with higher density ( $D_r = 48\%$ ), almost all of the active tensiometers show a drop in suction before the failure. In both categories of tests, at the lowest rainfall intensity (FLM\_06 for  $D_r = 34\%$  and FLM\_15 for  $D_r = 48\%$ ), no failure is observed despite a suction drop in all of the tensiometers. In tests with denser soil ( $D_r = 48\%$ ), initial suction varied in the range of 18.5–23.5 kPa.

Progress of wetting front loci with time is recorded throughout all of the flume tests (Fig. 11). Also, the failure surface is clearly observed from the side walls, and its depth is proved using inclinometer readings and analyzing images. Slope failures in all of the experiments show the mechanism of shallow, infinite-slope type movement, having failure surfaces nearly parallel to the surface of the slope. In all experiments under different rainfall regimes, the failure surface is almost planar, and its depth ranges between 10 and 20 cm from the ground surface (except in FLM\_12 in which a partly circular failure surface is observed). It should also be noted that in all flume

experiments, the deformations leading to a failure occurred almost instantaneously, i.e., they are not slowly developing movements visible in the soil, but they occur rather abruptly.

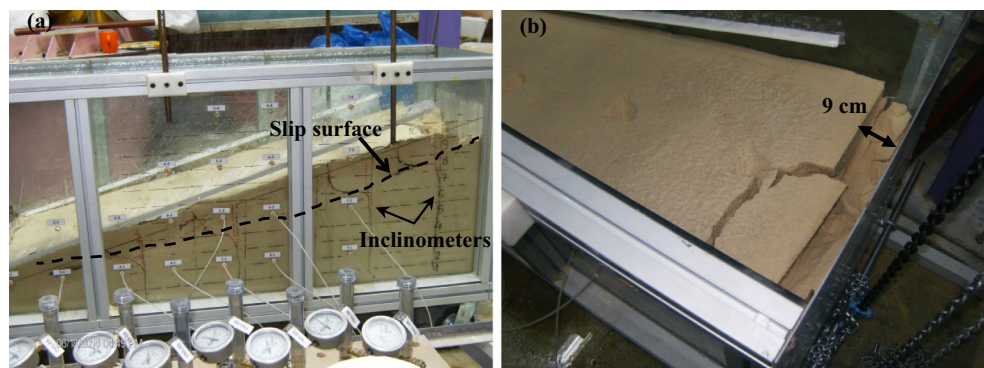
***I*–*D* threshold**

Plotting time to failure versus average rainfall intensity in flume experiments gives the rainfall *I*–*D* threshold that triggers a landslide. Figure 12 shows the *I*–*D* threshold for the two sets of tests with 34 and 48% relative density (see Table 3). Solid-filled symbols in Fig. 12 represent the experiments that have experienced failure, whereas the experiments in which no failure is observed till the end of the experiment are shown with data points with no filling (tests FLM\_06 and FLM\_15).

For each of the relative densities of  $D_r = 34\%$  and  $D_r = 48\%$ , a best fitting function is fitted to the data on the *I*–*D* plot. Overall, it is observed that the general shape of the *I*–*D* plot in log–log scale seems to be two-part linear in log–log scale. Considering the type of the function that is generally used in the literature for *I*–*D* thresholds as  $I = a \cdot D^{-b}$  (*I*: rainfall intensity, *D*: rainfall duration, and *a* and *b* are constants), the best fits are presented in power function format. The *a* values for 34 and 48% relative densities are obtained as 38 and 135, and *b* values are as 1.556 and 1.431, respectively. These values are in the vast range of common values for *a* (0–148), and *b* (0.1–2) reported in the literature (Giannecchini 2005; Aleotti 2004; Guzzetti et al. 2008; Ma et al. 2015, IRPI).

In FLM\_06 and FLM\_15 tests, failure is not observed until 295 and 355 min of continuous rainfall, respectively. When we plot the threshold rainfall intensity–duration curve, we wanted to show the experiments where we did not observe a failure, since these data points also provide useful information in drawing the boundary for the triggering-rainfall threshold. This may indicate having an asymptote-like lower limit to the *I*–*D* threshold. Current tests demonstrated physically that low intensity–long duration rainfalls and high intensity–short duration

**Fig. 8** FLM\_04 experiment **a** side view of the slipped block and slip surface and **b** top view showing the 9-cm translational movement at the slope crest



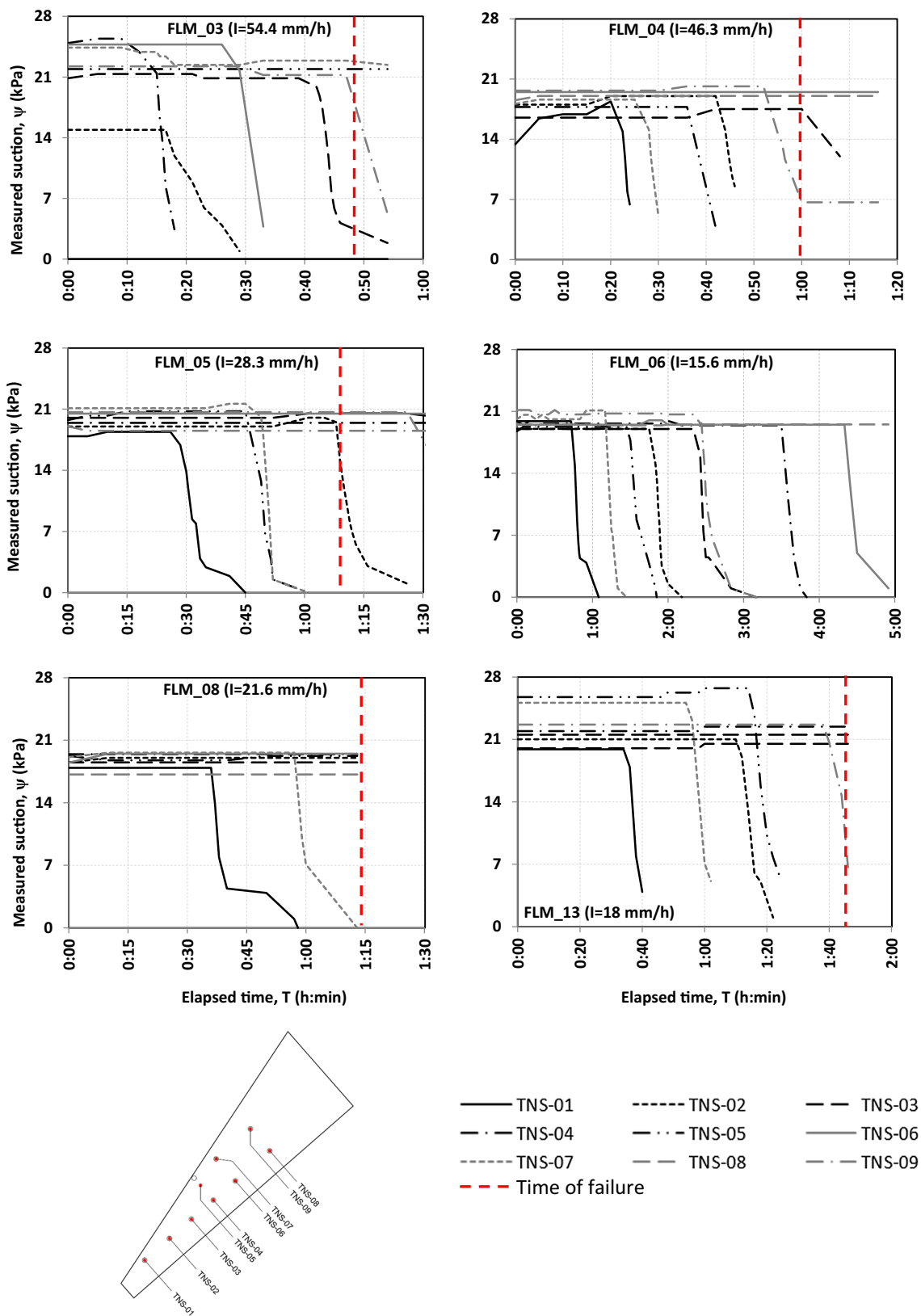
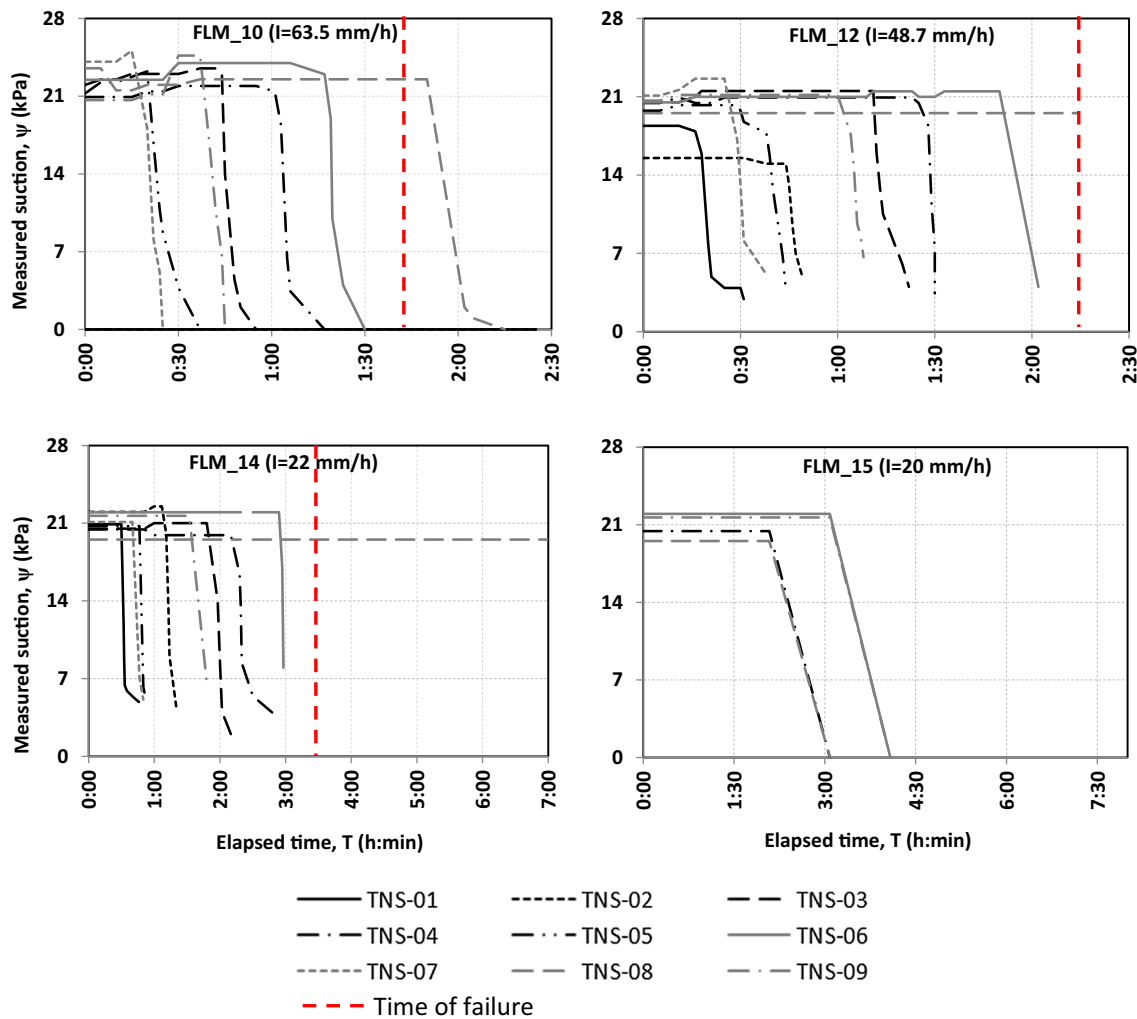


Fig. 9 Suction response after the start of rainfall at tests with  $D_r = 34\%$  (test number and rainfall intensity are indicated on each graph)



**Fig. 10** Suction response after start of constant rainfall for tests with  $D_r = 48\%$  (test number and rainfall intensity are indicated on each graph)

rainfalls can both trigger landslides (except the very small rainfall intensities, in the range of less than 15 mm/h for  $D_r = 34\%$  and 20 mm/h for  $D_r = 48\%$ ). For very low-intensity rainfalls, either the rainfall has to continue for a very long time to cause failure or it is impossible to cause failure in these very small values of rainfall intensity. The infiltration is at such a slow rate that the water can percolate through the entire depth of soil without forming a wetting front that would cause any slope instability. Limited number of other researchers, e.g., Cannon and Ellen (1985), Wieczorek (1987), Crosta and Frattini (2001) have also proposed asymptotic thresholds for long rainfall durations, or in other words, bilinear log–log intensity–duration relations (see Fig. 4).

The rainfall intensities applied in this study are in the range of 18–64 mm/h and rainfall duration ranges from less than 1 h to about 13 h. Although there is a limitation in these ranges as compared to real landslide-triggering rainfall events in different parts of the world, in different

slope angles and materials, they are within realistic ranges. The aim of the current study is, by no means, to propose an early warning threshold for a specific region. Instead, the main goal of this study is to trigger landslides by rainfall and obtain  $I$ – $D$  thresholds experimentally in the controlled-laboratory environment to investigate its shape and the effect of soil density on it.

### Conclusions

The major conclusions from the current research can be summarized as follows, for the rainfall-triggered landslides in the fine sand used in this study:

1. The failure surfaces are mostly translational, and failure mechanism is infinite-slope type landslide. The failure surface is generally coincident with the wetting front or is in its vicinity. As the rainfall infiltrates the soil, wetting front moves deeper and

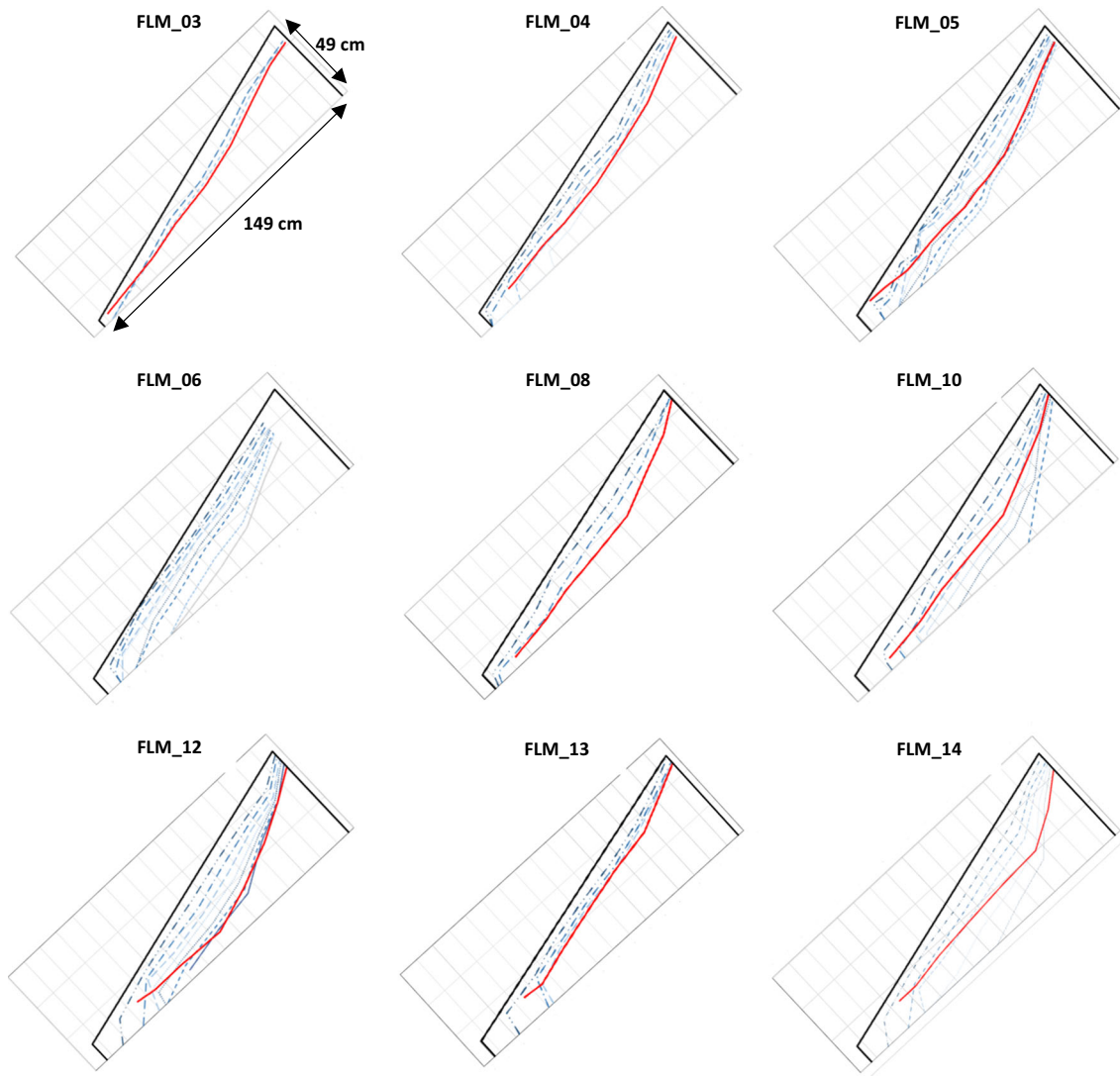


**Fig. 11** Movement of wetting front loci with time (blue dashed lines) throughout rainfall application and failure surface (red solid line)

**Fig. 12** Rainfall intensity–duration data from flume tests in this study

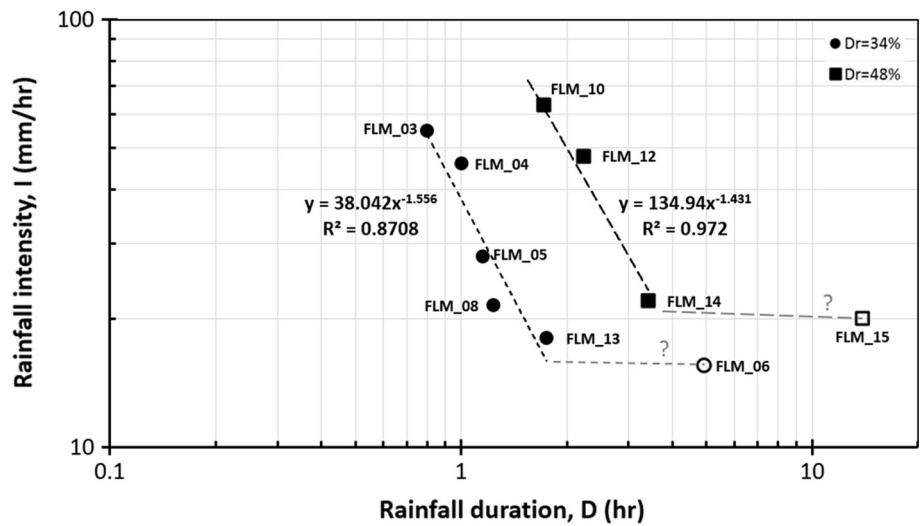


**Table 3** Time to failure in flume experiments

Test #	Rainfall intensity, <i>I</i> mm/h	Time to failure, <i>t</i> min	Test #	Rainfall intensity, <i>I</i> mm/h	Time to failure, <i>t</i> min
<i>D<sub>r</sub></i> = 34% (dry density 1.20 g/cm <sup>3</sup> )			<i>D<sub>r</sub></i> = 48% (dry density 1.27 g/cm <sup>3</sup> )		
FLM_03	54.4	48	FLM_10	63.5	103
FLM_04	46.3	60	FLM_12	48.7	134
FLM_05	28.3	69	FLM_14	22	205
FLM_06	15.6	No failure till 295 min	FLM_15	20	No failure till 355 min
FLM_08	21.6	74			
FLM_13	18	105			

causes a reduction in suction in the ground as it reaches the level of the tensiometer, starting from the tensiometers at shallower depths.

- In almost all flume experiments, the deformations leading to a failure occurred abruptly (in less than 3 s).
- The shape of the *I*–*D* threshold is demonstrated to be a bilinear relation in log–log plot of rainfall intensity versus duration. The results of this study confirm that both high intensity–short duration rainfalls and low intensity–long duration rainfalls can trigger landslides, and this can be demonstrated in laboratory physical tests.
- Below a certain rainfall intensity (in this study 15 and 20 mm/h for *D<sub>r</sub>* = 34% and *D<sub>r</sub>* = 48%, respectively), landslide is not triggered. This finding leads to a possible conclusion that the *I*–*D* relation could be asymptotic to a lower boundary of rainfall intensity. For such low-intensity rainfalls, either the rainfall has to continue for a very long time to cause failure or it is impossible to cause failure in these very small values of rainfall intensity. A plausible reason for this result is water entering at such a slow rate that it can be drained to the depths of the soil by gravity before it causes any slope instability at the surface.
- The effect of relative density of the soil on the *I*–*D* threshold is demonstrated by physical laboratory tests. As the relative density of the material increases, the triggering rainfall intensity–duration threshold line moves to larger rainfall events (in the log–log plot of intensity versus the duration).

In this study, rainfall intensity–duration threshold that would trigger a landslide is obtained and the effect of relative density of the soil on *I*–*D* threshold is demonstrated by physical model experiments in the laboratory for soil. All of the conclusions above are deduced for one type of soil (clean fine sand) used in this study, and that, any further studies would definitely strengthen the conclusions. The results of this study could be useful for future studies

on accurate numerical modeling of rainfall-triggered landslides.

**Acknowledgements** Funding for this research was provided by the Scientific and Technological Research Council of Turkey (TUBITAK) research Project No. 109M635.

**References**

Acharya G, Cochrane TA, Davies T, Bowman E (2009) The influence of shallow landslides on sediment supply: a flume-based investigation. *Eng Geol* 109:161–169

Ahmadi-adli M (2014) Shallow landslides triggered by rainfall in unsaturated soils. Ph.D. thesis, Middle East Technical University, Civil Engineering Department

Aleotti P (2004) A warning system for rainfall-induced shallow failures. *Eng Geol* 73:247–265

Alonso EE, Gens A, Josa A (1990) A constitutive model for partially saturated soils. *Geotechnique* 40(3):405–430

Askarinejad A (2013) Failure mechanism of unsaturated silty sand slopes triggered by rainfall. Ph.D. thesis, ETH Zurich

Caine N (1980) The rainfall intensity–duration control of shallow landslides and debris flows. *Phys Geogr* 62(1/2):23–27

Cannon SH, Ellen SD (1985) Rainfall conditions for abundant debris avalanches, San Francisco Bay region, California. *Calif Geol* 38:267–272

Cannon SH, Gartner JE (2005) Wildfire-related debris flow from a hazards perspective. In: Jakob M, Hungr O (eds) *Debris flow hazards and related phenomena*. Springer, Berlin, pp 363–385

Chen Z, Wang J (2007) Landslide hazard mapping using logistic regression model in Mackenzie Valley. *Can Nat Hazards* 42(1):75–89

Clarizia M, Gullà G, Sorbino G (1996) Sui meccanismi di innesco dei soil slip. *Int Conf Prev Hydrogeol Hazards Role Sci Res* 1:585–597 (in Italian)

Crosta G, Frattini P (2001) Rainfall thresholds for triggering soil slips and debris flow. In: Mugnai A, Guzzetti F, Roth G (eds) *Proceedings of the 2nd EGS plinius conference on mediterranean storms*, Siena, pp 463–487

Crosta G, Frattini P (2003) Distributed modelling of shallow landslides triggered by intense rainfall. *Nat Hazards Earth Syst Sci* 3:81–93

Damiano E (2004) Mechanisms of triggering mudslides in pyroclastic soils. Ph.D. thesis, Aversa, Second University of Napoli (in Italian)

- Eichenberger J, Ferrari A, Laloui L (2013) Early warning thresholds for partially saturated slopes in volcanic ashes. *Comput Geotech* 49:79–89
- Fang H, Cui P, Pei LZ, Zhou XJ (2012) Model testing on rainfall-induced landslide of loose soil in Wenchuan earthquake region. *Nat Hazards Earth Syst Sci* 12:527–533
- Gianneccini R (2005) Rainfall triggering soil slips in the southern Apuane Alps (Tuscany, Italy). *Adv in Geosci* 2:21–24
- Godt JW, Baum RL, Lu N (2009) Landsliding in partially saturated materials. *Geophys Res Lett* 36(L02403):1–5
- Guzzetti F, Peruccacci S, Rossi M, Stark CP (2007) Rainfall thresholds for the initiation of landslides in central and southern Europe. *Meteorol Atmos Phys* 98(3–4):239–267
- Guzzetti F, Peruccacci S, Rossi M, Stark CP (2008) The rainfall intensity–duration control of shallow landslides and debris flows: an update. *Landslides* 5:3–17
- Hong Y, Adler R, Huffman G (2006) Evaluation of the potential of NASA multi-satellite precipitation analysis in global landslide hazard assessment. *Geophys Res Lett* 33:L22402. doi:10.1029/2006GL028010
- Huang C-C, Yuin S-C (2010) Experimental investigation of rainfall criteria for shallow slope failures. *Geomorphology* 120:326–338
- Innes JL (1983) Debris flows. *Progr Phys Geogr* 7:469–501
- IRPI, Rainfall thresholds for the initiation of landslides. [http://www.db.gndci.cnr.it/php2/rainfall\\_thresholds/thresholds\\_all.php?lingua=it](http://www.db.gndci.cnr.it/php2/rainfall_thresholds/thresholds_all.php?lingua=it). Accessed 12 Feb 2017
- Iverson RM, Reid ME, La Husen RG (1997) Debris-flow mobilization from landslides 1. *Annu Rev Earth Planet Sci* 25(1):85–138
- Jibson RW (1989) Debris flow in southern Porto Rico. *Geol Soc Am Spec Pap* 236:29–55
- Lourenco S, Sassa K, Fukuoka H (2006) Failure process and hydrologic response of a two layer physical model: implications for rainfall-induced landslides. *Geomorphology* 73:115–130
- Lu N, Godt JW (2013) Hillslope hydrology and stability. Cambridge University Press, Cambridge
- Lu N, Sener-Kaya B, Wayllace A, Godt JW (2012) Analysis of rainfall-induced slope instability using a field of local factor of safety. *Water Resour Res* 48:W09524
- Ma T, Li C, Lu Z, Bao Q (2015) Rainfall intensity–duration thresholds for the initiation of landslides in Zhejiang Province, China. *Geomorphology* 245:193–206
- Montgomery DR, Dietrich WE, Torres R (1997) Hydrologic response of a steep, unchanneled valley to natural and applied rainfall. *Water Resour Res* 33(1):91–109
- Montrasio L, Valentino R (2007) Experimental analysis and modelling of shallow landslides. *Landslides* 4(3):291–296
- Moriwaki H, Inokuchi T, Hattajji T, Sassa K, Ochiai H, Wang G (2004) Failure processes in a full-scale landslide experiment using a rainfall simulator. *Landslides* 1:277–288
- Nadim F, Cepeda F, Sandersen F, Jaedicke C, Heyerdahl H (2009) Prediction of rainfall-induced landslides through empirical and numerical models. In: Proceedings of IWL—the first Italian workshop on landslides, Naples, 8/10 June 2009, vol 1, pp 206–215
- Okada Y (2014) Changes in shear strain and subsurface flow prior to rainfall-induced landslide in 15 flume experiments. In: Sassa K, Canuti P, Yin Y (eds) *Landslide science for a safer geoenvironment*. Springer, Cham, pp 81–86
- Okura Y, Kitahara H, Ochiai H, Sammori T, Kawanami A (2002) Landslide fluidization process by flume experiments. *Eng Geol* 66:65–78
- Olivares L, Damiano E, Greco R, Zeni L, Picarelli L, Minardo A, Guida A, Bernini R (2009) An instrumented flume to investigate the mechanics of rainfall-induced landslides in unsaturated granular soils. *Geotech Test J* 32(2):1–11
- Orense RP, Shimoma S, Maeda K, Towhata I (2004) Instrumented model slope failure due to water seepage. *J Nat Disaster Sci* 26:15–26
- Picarelli L, Olivares L, Damiano E (2006) Discussion to “evaluation of landslide triggering mechanisms in model fill slopes” by W.A. Take, M.D. Bolton, P.C.P. Wong, and F.J. Yeung [*Landslides* 1(3):173–184, October 2004] and “A fluidized landslide on a natural slope by artificial rainfall” by H. Ochiai, Y. Okada, G. Furuya, Y. Okura, T. Matsui, T. Sammori, T. Terajima, and K. Sassa [*Landslides* 1(3):211–219 (October 2004)]. *Landslides* 3(3):269–272
- Rahardjo H, Leong EC, Rezaur RB (2008) Effect of antecedent rainfall on pore water pressure distribution characteristics in residual soil slopes under tropical rainfall. *Hydrol Processes* 22:506–523
- Rahimi A, Rahardjo H, Leong E-C (2011) Effect of antecedent rainfall patterns on rainfall-induced slope failure. *J Geotech Geoenviron Eng* 137(5):483–491
- Reichenbach P, Cardinali M, De Vita P, Guzzetti F (1998) Regional hydrological thresholds for landslides and floods in the Tiber River Basin (central Italy). *Environ Geol* 35(2):146–159
- Richards LA (1931) Capillary conduction of liquids through porous mediums. *Physics* 1(5):318–333
- Rossi M, Guzzetti F, Reichenbach P, Mondini AC, Peruccacci S (2010) Optimal landslide susceptibility zonation based on multiple forecasts. *Geomorphology* 114:129–142
- Schnellmann R, Busslinger M, Schneider HR, Rahardjo H (2010) Effect of rising water table in an unsaturated slope. *Eng Geol* 114:71–83
- Springman SM, Thielen A, Kienzler P, Friedel S (2013) A long-term field study for the investigation of rainfall-induced landslides. *Geotechnique* 63(14):1177–1193
- Take WA, Bolton MD, Wong PC, Yeung FJ (2004) Evaluation of landslide triggering mechanisms in model fill slopes. *Landslides* 3(1):173–184
- Tohari A, Nishigaki M, Komatsu M (2007) Laboratory rainfall-induced slope failure with moisture content measurement. *J Geotech Geoenviron Eng* 133(5):575–587
- Toll DG, Lourenco SDN, Mendes J, Gallipoli D, Evans FD, Augarde CE, Cui YJ, Tang AM, Rojas JC, Pagano L, Mancuso C, Zingariello C, Tarantino A (2011) Soil suction monitoring for landslides and slopes. *Q J Eng Geol Hydrogeol* 44(1):23–33
- Van Westen CJ (2007) Mapping landslides: recent developments in the use of digital information. In: Proceedings of the first North American conference on landslides, Vail, pp 221–238
- Vennari C, Gariano SL, Antronico L, Brunetti MT, Iovine G, Peruccacci S, Terranova O, Guzzetti F (2014) Rainfall thresholds for shallow landslide occurrence in Calabria, southern Italy. *Nat Hazards Earth Syst Sci* 14:317–330
- Wang G, Sassa K (2001) Factors affecting rainfall-induced flowslides in laboratory flume tests. *Geotechnique* 51(7):587–599
- Wang G, Sassa K (2003) Pore-pressure generation and movement of rainfall-induced landslides: effects of grain size and fine-particle content. *Eng Geol* 69:109–125
- Wieczorek GF (1987) Effect of rainfall intensity and duration on debris flows in central Santa Cruz Mountains. In: Costa JE, Wieczorek GF (eds) *Debris flow/avalanches: process, recognition, and mitigation*. Reviews in Engineering Geology, vol 7. Geological Society of America, Boulder, pp 93–104
- Wu LZ, Huang RQ, Xu Q, Zhang LM, Li HL (2015) Analysis of physical testing of rainfall-induced soil slope failures. *Environ Earth Sci* 73:8519–8531
- Zhou J, Li YX, Jia MC, Li CN (2013) Numerical simulation of failure behavior of granular debris flows based on flume model tests. *Sci World J* 2013:10. doi:10.1155/2013/603130